

Circumferential twist in flow forming of tubular parts: Characterization, understanding and control

P.F. Gao^{a,b}, M. Li^a, M.W. Fu^b, M. Zhan^{a,*}, L. Xing^a, F. Ma^c

^a State Key Laboratory of Solidification Processing, Shaanxi Key Laboratory of High-Performance Precision Forming Technology and Equipment, School of Materials Science and Engineering, Northwestern Polytechnical University, P.O. Box 542, Xi'an 710072, PR China

^b Department of Mechanical Engineering, The Hong Kong Polytechnic University, Hung Hom, Kowloon, Hong Kong, PR China

^c Long March Machinery Factory, China Aerospace Science and Technology Corporation, Chengdu, 610100, China

*Corresponding author. Tel. /fax: +86-029-8849-5632. E-mail address: zhanmei@nwpu.edu.cn

Abstract

Flow forming and flattening of welded tube provides a feasible way to form integral ultra-wide blanks. The weld line deflection in flow forming, however, limits the effective size and material utilization rate of the final integral blank. In this study, the characterization, mechanism and control of weld line deflection are investigated via finite element (FE) simulation and experiment. First, a FE model considering the difference of deformation behavior between weld and parent metal is established and validated for flow forming of an aluminum alloy welded tube. Both the simulation and experiment results show that the weld line is deflected to a helix with the helix orientation being contrary to that of the helical trajectory of roller on workpiece. This weld deflection is a combined result of the shear deformation in θ - z and r - θ planes (θ -circumferential, r -radial, z -axial) in forming region. The shear deformation in θ - z plane is nearly the simple shear mode, which is the essential reason for weld line deflection. The shear strain $\varepsilon_{\theta z}$ is almost equal to the helix angle of deflected weld line, which is defined as the deflection angle for evaluation of the deflection degree. The shear deformation in r - θ plane ($\varepsilon_{r\theta}$) results in a little difference on the circumferential deflection distance between the inner and outer surface of tube, but makes a little bit difference on the deflection angles of two surfaces. Reduction (ψ_t) and feed rate (f) are the first and second significant factor for deflection angle, respectively. $\varepsilon_{\theta z}$ and deflection angle are increased with ψ and f . To convert the deflected weld line to straight, conducting spinning pass with an opposite mandrel rotation direction to the first pass is feasible. However, rigorous processing design is required to adjust to the deflection angle, which is a

difficult and tedious process. To this end, a new method by applying circumferential constraint on workpiece is proposed to control the deflection, which possesses higher efficiency and better universality. On the other hand, it is interesting to find that the circumferential deflection is an intrinsic phenomenon in the flow forming of tubes, whether there exists the weld line or not. It means that the above results provide well explanation and control method for the intrinsic circumferential deflection (or called as twisting) in the flow forming.

Too tedious and did not give the impact! Why you need to do this rsearch?

Keywords: Welded tube; Flow forming; Weld line deflection; Deflection mechanism, Control method

1. Introduction

With the rapid developments of high-end equipment in aerospace, the scales of its key components are getting larger and larger to satisfy the demands of large capacity and long range. For example, the aluminum alloy large-scale head of pressure vessels in the latest heavy lift launch vehicle is greater than 5m. The integral plastic forming process, such as spinning, presents unique advantages of high quality, simple tooling, and high efficiency to form these components (Kwiatkowski et al., 2013). However, it is difficult to obtain high quality initial integral blank with large size in this order by rolling directly, which limits the high-performance plastic forming of these large-scale components. Fortunately, a three-step integrated process with coil welding, flow forming and flattening provides a feasible way to form the large-scale integral blank. In this process, the thick plate is first coil welded into a welded tube, then flow formed getting thinner and longer, and finally cut along the weld line and flatten to blank, as shown in Fig. 1. Specially, flow forming of welded tube is the most crucial step, which greatly determine the geometrical size and forming quality of the final blank.

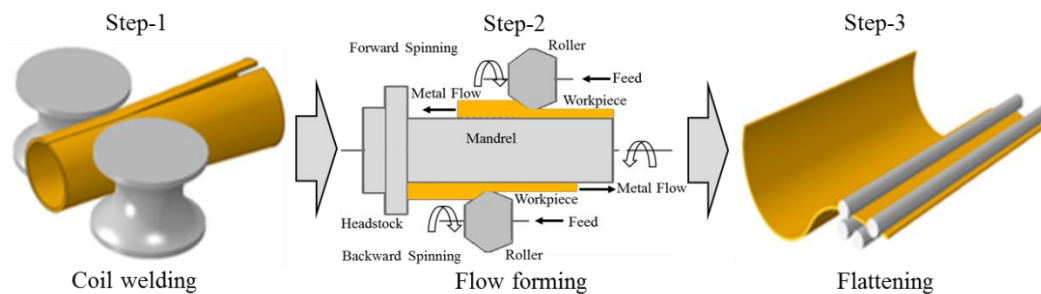


Fig. 1 The schematic of three-step integrated process with coil welding, flow forming and flattening for forming large-scale integral blank.

In the flow forming of tube, the material undergoes complicated axial and circumferential deformation, which makes the workpiece generate a certain degree of twisting while being elongated

(Mohebbi et al., 2010). For welded tube, this may result in the weld line deflection, which then determines the geometry of blank after cutting and flattening. Serious deflection will cause a reduction in material utilization rate and limit the effective size of produced integral blank. Essentially, the deflection characteristics and degree are related to the axial and circumferential deformation behaviors, which are greatly affected by the material and processing parameters. In addition, the different deformation behaviors between weld and parent metal may intensify the deformation inhomogeneity and affect the axial and circumferential deformation behaviors. This may further bring complex effects on the weld line deflection. Therefore, it is critical to investigate the formation mechanism and control method of weld line deflection in the flow forming of welded tube.

At present, there have been lots of researches conducted on the deformation characteristics during flow forming. It has been reported that the forming region is subjected to three-dimensional compressive stress during flow forming (Zhang et al., 2017). The material mainly undergoes compression deformation in the radial direction and tensile deformation in the axial and circumferential directions (Mohebbi et al., 2010). Shinde et al. (2016) developed a FE model and investigated the effects of processing parameters on the plastic stress, strain and spinning force in the flow spinning of maraging steel tube. Xu et al. (2016) found that the non-uniform roller distribution will lead to the non-periodic variation of stress distribution along circumferential direction in flow forming. And, the number of roller and the included angle between them have a significant influence on the spinning force. Xue et al. (2001) investigated the dependence of circumferential strain on flow forming parameters and found that the circumferential deformation degree increases with the decrease of roller attack angle and the increases of feed ratio, blank wall thickness and reduction rate. However, little of these works focus on the mechanism and rules of tube twisting in flow forming. Moreover, the uneven material properties of welded tube may lead to different deformation characteristics and more complex twisting behavior compared to the above works on homogeneous tube.

On the other hand, some works have been conducted on the deformation characteristics and weld line movement in the plastic forming of tailor welded blank. Heo et al. (2001) characterized the weld line movement in the deep drawing of SPC1 alloy tailor welded blank, and quantitatively investigated the effect of drawbead dimension on the weld line movement. Liu et al. (2016) and Wang et al. (2017) studied the weld line movement and strain distribution under different forming conditions in the hot stamping of AA6082 tailor welded blanks. It is concluded that the movement displacement of weld line

increases with the thickness ratio increasing. Zhang (2012) has investigated the influences of forming temperature, radius of the concave and convex mold, friction coefficient and clamping gap on weld line movement in V-shaped free bending. However, the characteristics of deformation and weld line movement in flow forming are quite different from those in stamping and deep drawing. Thus, it is needed to conduct deep investigations on the characterization, formation mechanism and control method of weld line deflection in the flow forming of welded tube.

In this study, a FE model considering the difference in deformation behavior between weld and parent metal was first developed and validated for the flow forming of an aluminum alloy welded tube. Then, the weld line deflection characteristics, mechanisms and their dependences on the processing parameters were quantitatively analyzed. Moreover, two control methods with different ideas for the weld line deflection were proposed and compared. The results will deepen the understanding on weld line deflection and provide guidance for its control in the flow forming of welded tube.

2. FE model and experiment of flow forming of welded tube

To reveal the mechanisms and rules of weld line deflection in flow forming of welded tube, FE simulation was employed, as it can conveniently reveal the instantaneous deformation and flow of material (Fu, 2016). In this section, the FE modelling of flow forming of an aluminum alloy welded tube and its experimental validation is described.

2.1 FE modelling

In this work, a 3D-elastic-plastic FE model of flow forming of welded tube was established, as shown in Fig. 2. The blank is the 2219 aluminum alloy welded tube by the friction stir welding. The distribution of weld line is shown in Fig. 2, whose width is determined to be 14mm through microhardness and metallographic tests. The constitutive behaviors of parent metal and weld were measured through the tensile test and well fitted by Hollomon equation (eq. (1)):

$$\sigma = K\varepsilon^n \quad (1)$$

where K is strengthening coefficient, n is hardening exponent. Table 1 lists the determined material parameters of parent metal and weld, which were input into the FE model. The local cylindrical coordinate system (radial- r , circumferential- θ , axial- z) is set to define material orientation and describe the deformation state and material flow. The welded tube is set as a deformable body and meshed by an 8-node reduced integration brick element. Four layer elements are adopted along the thickness

direction of tube blank, which are sufficient to model the deformation characteristics in thickness direction during flow forming (Yang et al., 2010). The roller and mandrel are set as rigid body. The Coulomb's friction model is used to represent the friction between tube blank and tools. The friction coefficients between blank and mandrel, and blank and roller are set as 0.1 and 0.05, respectively. During flow forming, the tube blank is tied with the mandrel at the bottom end. While, two rollers counterclockwise revolves around the workpiece and feed at a constant speed along the axial direction at the same time. Thus, the movement trajectory of roller on workpiece is a right-handed helix, as indicated by the black line in Fig.2. The detailed forming parameters are given in Table 2.

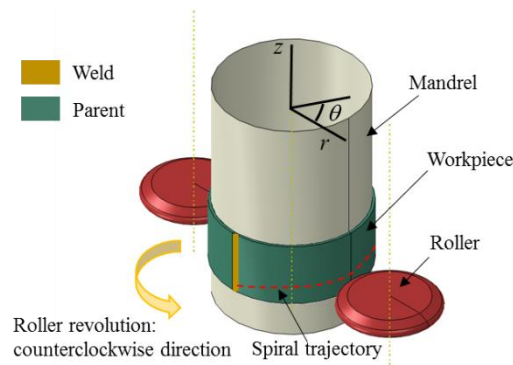


Fig. 2 3D elastic-plastic FE model for flow forming of welded tube.

Table 1 Material parameters of parent metal and weld in 2219 aluminum alloy welded tube.

Parameter	Parent metal	Weld
Young's modulus E (MPa)	57087	62884
Yield strength σ_s (MPa)	86.67	79.63
Strengthening coefficient K (MPa)	252.86	355.27
Hardening exponent n	0.165	0.216

Table 2 Detailed forming parameters in FE model and experiment.

Forming parameters	Values
Blank	
Inner diameter (mm)	324
Wall thickness (mm)	6
Initial length (mm)	110
Roller	
Roller fillet radii (mm)	10
Attack angle α_R ($^\circ$)	30
Smoothing angle ($^\circ$)	60
Forming conditions	
Feed rate f (mm/r)	1
Reduction ψ_t (%)	25
Rotation speed (r/min)	90

2.2 Experimental validation of FE model

In order to verify the reliability of FE model, the flow forming experiment of welded tube was conducted on a CZ900/2CNC spinning machine, as shown in Fig. 3. The forming parameters in experiment are the same as those in FE simulation (Table 2). It should be noted that the relative rotation between roller and workpiece is realized by the clockwise rotation of workpiece in experiment, which is different to the revolution of rollers in FE model. However, the helical trajectory of roller on workpiece is the same for two conditions.

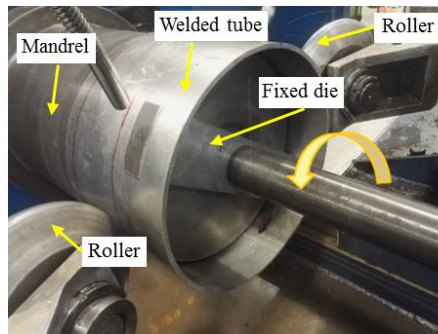


Fig. 3 Set-up for flow forming experiments on a CZ900/2CNC spinning machine.

Fig. 4 shows the comparison of spun tubes obtained by experiment and simulation. It can be seen that the deformed weld shapes (indicated by red lines) in experiment and simulation are very close. Besides, the weld line movement was quantitatively evaluated by its circumferential deflection distance relative to the initial position. Here, looking from top to bottom, the counterclockwise deflection direction is defined as the positive direction. Fig. 5(a) shows the measured deflection distances of inner and outer surfaces of tube at different axial heights. The average relative errors between experimental and simulated deflection distance of the inner and outer surfaces are 4.58% and 3.59%, respectively. In addition, the wall thickness distribution along the circumferential direction in a circle was also measured and compared in Fig. 5(b). It can be seen that the wall thickness distribution in simulation is very close to the experiment result with the maximum relative error of 1.86%. These comparisons prove that the established FE model is reliable, which can be employed to investigate the mechanism and rules of weld line deflection.

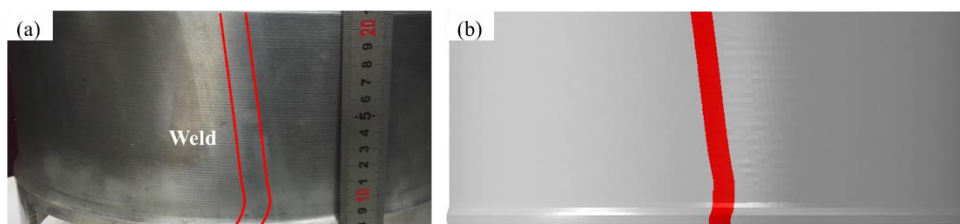


Fig. 4 Spinning formed welded tubes: (a) experimental result; (b) FE simulation result.

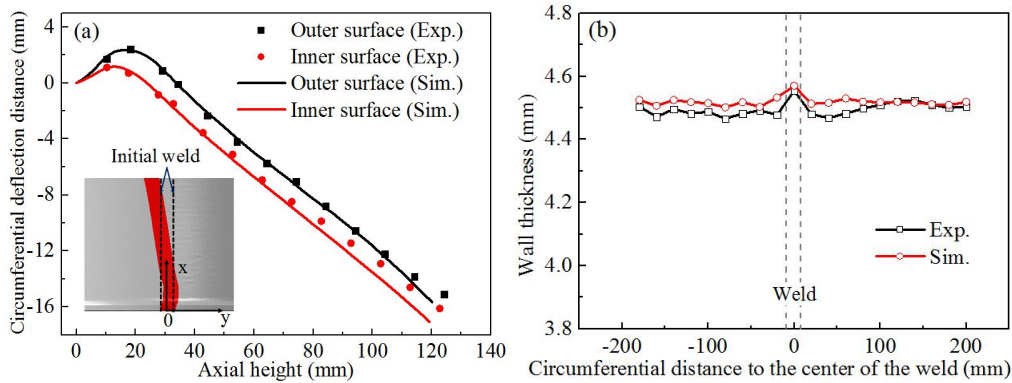


Fig. 5 Comparisons of the circumferential deflection distance of weld line (a) and wall thickness distribution (b) between experimental and FE simulation results.

3. Weld line deflection in the flow forming of welded tube

In this section, the point tracking method is applied to capture the development process and characteristics of weld line deflection. The shape and degree of deflected weld line are described. Moreover, underlying mechanism of deflection is revealed by analyzing the deformation characteristics during flow forming.

3.1 Deflection characteristics

The tracked points distribute at the middle axial section of weld at a certain axial height, as shown in Fig. 6(a). Their circumferential displacement variations with forming time are given in Fig. 6(b). It can be divided into three stages: unformed stage, forming stage and formed stage, which right correspond to the tracked points locating in unformed region, forming region and formed region (shown in Fig. 7), respectively. In the unformed stage, the tracked points move along the negative direction and their displacements gradually increase with forming process at a constant speed v , as shown in Fig. 6(b). And, the points at different thickness present little difference on deflection displacements. Meanwhile, it can be found from Fig. 7 that the weld line is a vertical line in the unformed region, whose deflection distance keeps constant with the variation of axial height. These indicate that the weld line in unformed region deflects along the negative direction as a whole, which is opposite to the direction of roller revolution. When the points enter the forming stage, i.e., the forming region, the negative deflection displacement keeps increasing and reaches to the maximum value in the early stage, where the growth rate gets smaller and smaller. Then, the movement direction of these points changes to the positive

direction, which means the deflection distance decreases to some extent. In addition, the displacement change in positive direction gradually decreases from the outer surface to inner surface and approaches 0 at the inner surface. The weld line in forming region is a tilted line connecting the unformed region and formed region, as shown in Fig. 7. In the formed stage, the tracked points locate in the formed region. Their movements are not affected by the roller loading action and keep constant, as shown in Fig. 6(b).

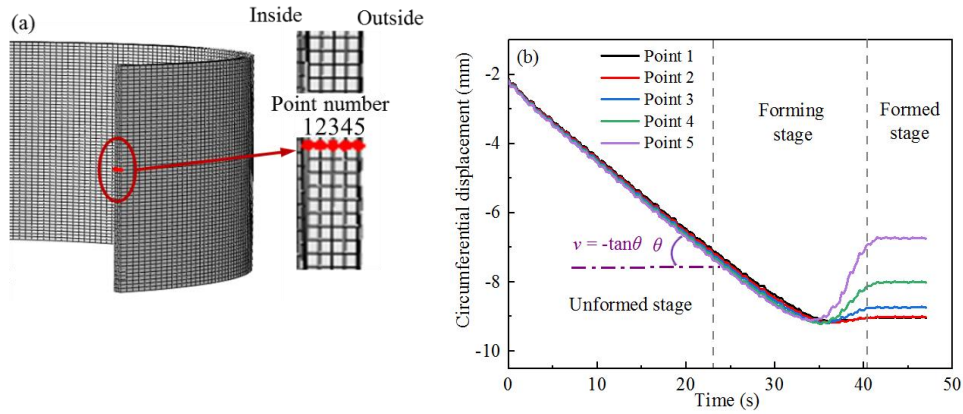


Fig. 6 Schematic of the position of tracked points (a) and their circumferential displacement variation during forming process (b).

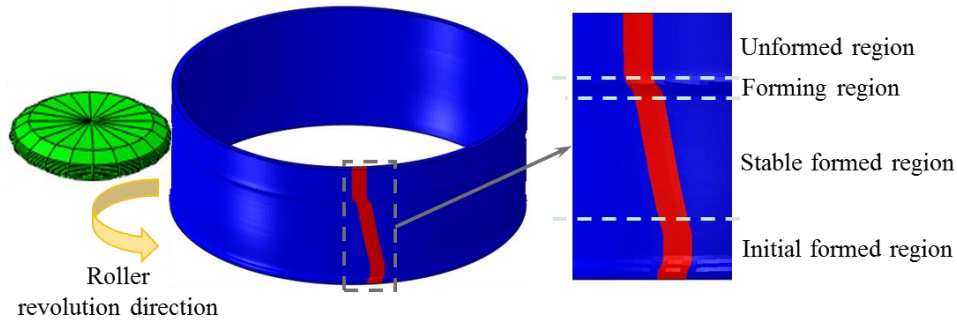


Fig. 7 The weld shape at a typical moment during the flow forming.

Fig. 8 shows the variation of circumferential deflection distance of the final deformed weld line, i.e., the weld line in stable formed region, with axial height. It can be seen that the deflection distances at outer and inner surfaces both increases linearly with the axial height, which suggest that the deformed weld line become a helix. The helix angle α is defined as deflection angle to evaluate the deflection degree in this work. In addition, it also can be seen that the deflection distance of the inner surface is ΔS larger than that of the outer surface. While, deflection angles of inner and outer surface are the same, which is inferred from the same slopes of two lines in Fig. 8.

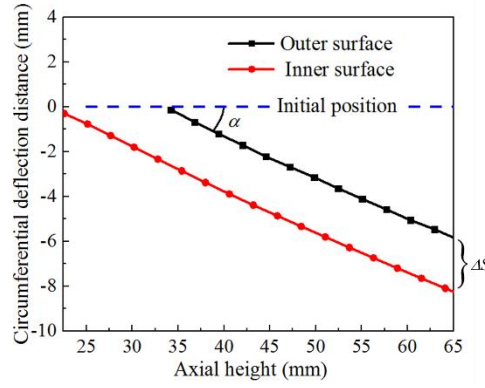


Fig. 8 Variation of the circumferential deflection distance with axial height in the stable formed region.

From the above analyses, it can be concluded that the deflection was mainly displayed in the opposite rotation of unformed region relative to the direction of roller revolution (Fig. 2). However, this is a rigid rotation of free end in workpiece without any accelerated speed, which indicates that it is a passive movement. Actually, the deflection stems from the deformation in forming region, which will be explained in detail in Section 3.2. In the formed region, the weld line does not move any more. Ultimately, the deformed weld line becomes a helix with the helix orientation being contrary to that of helical trajectory of roller. And the deflection distance at inner surface is a little larger than that of the outer surface, while, the deflection angles of weld line at inner and outer surfaces are the same.

3.2 Deflection mechanisms

As described in Section 1, the forming region is mainly subjected to three-dimensional compressive stress, and whose deformation state is usually simplified as the compression strain in the radial direction and tensile strain in the axial and circumferential directions during flow forming (Xu et al. 2001). In practice, there is still considerable shear deformation in $r-\theta$, $r-z$ and $\theta-z$ planes, which may also affect the forming results. Shan et al. (2009) found that the combination of shear and compression deformation results in the distorted grain morphology in flow forming of TA15 titanium alloy. In addition, Wang et al. (2018) revealed that the shear deformation in $r-\theta$ and $r-z$ planes can promote the grain refinement. However, the effect of shear deformation on the macro forming characteristics have not attracted enough attentions. From geometry, the shear strain $\varepsilon_{\theta z}$ in $\theta-z$ plane is related to the deformation on plane of deflection, which may be responsible for the deflection of weld line. Thus, the evolution of shear strain $\varepsilon_{\theta z}$ of a point on the inner surface (Point 1) and a point on the outer surface (Point 5) in Fig. 6(a) during flow forming were tracked and given in Fig. 9. It can be seen from Fig. 9 that $\varepsilon_{\theta z}$ keeps 0 in the unformed stage. In the forming stage, the material first undergoes a negative

shear deformation process reaching a large shear strain $-\Delta_1$ in the early stage. While, an opposite shear deformation process with the shear strain of Δ_2 a little smaller than Δ_1 is followed, which will offset the early negative shear strain to some extent. Finally, a negative $\varepsilon_{\theta z}$ ($\Delta_2 - \Delta_1$) is generated after forming stage and does not vary any more in the formed stage.

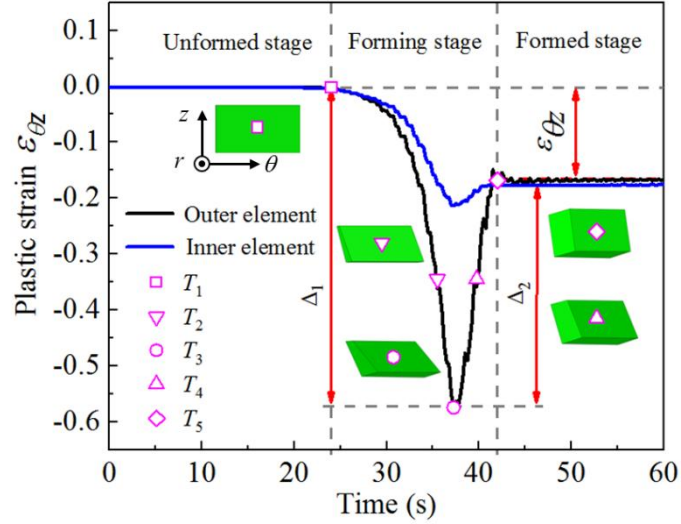


Fig. 9 Evolutions of $\varepsilon_{\theta z}$ and element shape of tracked points during the flow forming process.

To graphically understand the evolution of $\varepsilon_{\theta z}$, the shape variation of typical element at the outer surface is also shown in Fig. 9 as an example. It is observed along the negative r -axis at five typical times ($T_1 \sim T_5$ in Fig. 9). It can be found that the element distorts from a rectangle to a parallelogram in θ - z plane during the forming stage. Similar to the variation trend of $\varepsilon_{\theta z}$, the distortion degree first increases and then decreases to some extent. Besides, it can be seen that the top and bottom sides of element nearly keeps horizontal in the whole process, which suggests that the shear deformation in θ - z plane is close to the simple shear mode (Thiel et al., 2019). The final shear angle β (depicted in Fig. 10) is approximately equals to the $\varepsilon_{\theta z}$ (0.16) after forming stage. Moreover, it is interesting to note that they are right equal to the deflection angle of weld line (0.14, expressed in radian). Their equality relation indicates that the approximate simple shear deformation in θ - z plane is right the underlying reason for the deflection of weld line.

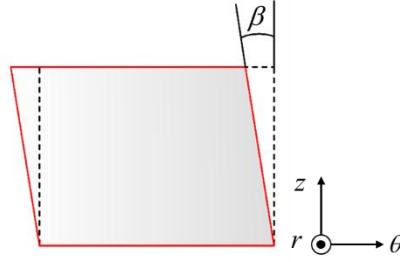


Fig. 10 The shear angle β of final element shape in Fig. 9.

As described above, the material experiences two stages of shear deformation in two opposite directions during forming stage. This means that there exist two feature regions presenting different deformation characteristics in the rolling action region, i.e., the forming region. Fig. 11 illustrates the contour of increment of $\varepsilon_{\theta z}$ ($\Delta\varepsilon_{\theta z}$) in a short time in the roller action region, which corresponds to the process of a roller moving from Position A to Position B. It can be seen that the material in front of roller (Region 1) undergoes a negative $\varepsilon_{\theta z}$, while the material under roller (Region 2) undergoes a positive $\varepsilon_{\theta z}$. The negative shear deformation in Region 1 just drives the unformed region rotating rigidly and then generates the deflection of weld line. In Region 2, the positive shear deformation occurs, which reduces the magnitude of $\varepsilon_{\theta z}$ (Fig. 9) and the circumferential displacement of weld line (Fig. 6) to some extent.

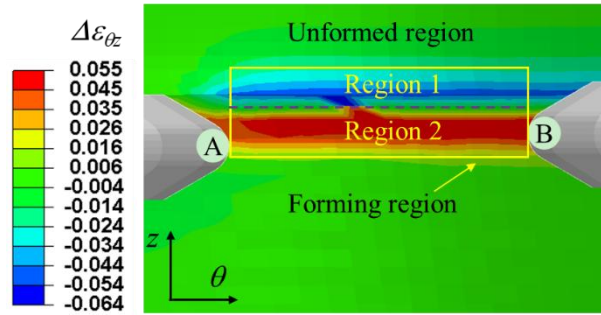


Fig. 11 Increment of $\varepsilon_{\theta z}$ contour in the roller action region. A-the initial position of roller, B-the end position.

Another hand, we can find from Fig. 9 that the shear deformation degrees of two stages Δ_1 and Δ_2 at outer surface are both greater than those at inner surface, however, the final $\varepsilon_{\theta z}$ after forming stage varies little with the thickness position. Thus, it can not explain the difference of deflection distance between the inner and outer surfaces (ΔS in Fig. 8). To reveal the reason, the deformation and shear strain $\varepsilon_{r\theta}$ in the r - θ section across the weld line were analyzed, as shown in Fig. 12. It can be seen that a significant shear deformation is produced and the shear strain $\varepsilon_{r\theta}$ decreases from the outer surface to

the inner surface gradually. Compared with the initial element geometry (gray dotted line), the elements are greatly inclined by the shear deformation. Considering the circumferential position, the outer surface deviates 2.24mm relative to the inner surface after deformation, which is exactly close to the above ΔS (2.44mm). Therefore, it can be concluded that the difference of deflection distance between inner and outer surfaces is attributed to the shear deformation in r - θ section ($\varepsilon_{r\theta}$).

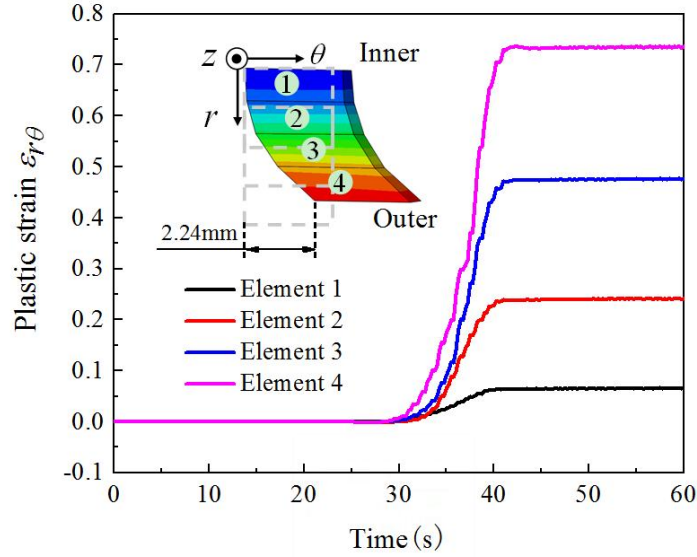


Fig. 12 Deformation and shear strain $\varepsilon_{r\theta}$ in the r - θ section across weld line.

The above analyses suggest the weld line deflection are caused by the synthetical effects of shear deformation in θ - z and r - θ planes. The simple shear deformation in θ - z plane in the forming region is the essential reason for the weld line deflection. The final deflection angle nearly equals to the shear strain $\varepsilon_{\theta z}$, which is the result of two stages of shear deformation in the opposite directions. Besides, the shear deformation in r - θ plane ($\varepsilon_{r\theta}$) results in the difference of deflection distance between the inner and outer surfaces. While, the deflection angles of weld line at inner and outer surfaces are the same.

On the other hand, the flow forming of homogeneous tube without weld was also conducted as comparison to investigate the influence of inhomogeneous material on deflection. Fig. 13 shows the circumferential displacement of tracked points on both of homogeneous and welded tubes. It can be found that their curves are nearly the same, which suggests that the existence of weld line has little effect on the circumferential flow of material. This is because the weld is very narrow relative to the parent metal for large diameter tube. The effect of different material properties of weld on the circumferential deformation characteristic of the whole tube can be negligible. Moreover, we can draw a conclusion that the circumferential deflection is an intrinsic phenomenon in the flow forming, which

is right the twisting observed by [Mohebbi et al., \(2010\)](#). It is just obviously displayed as the deflection of weld line in the flow forming of welded tubes. That is to say, the circumferential deflection (or called as twisting), an intrinsic phenomenon in the flow forming of tube, is well explained in this work.

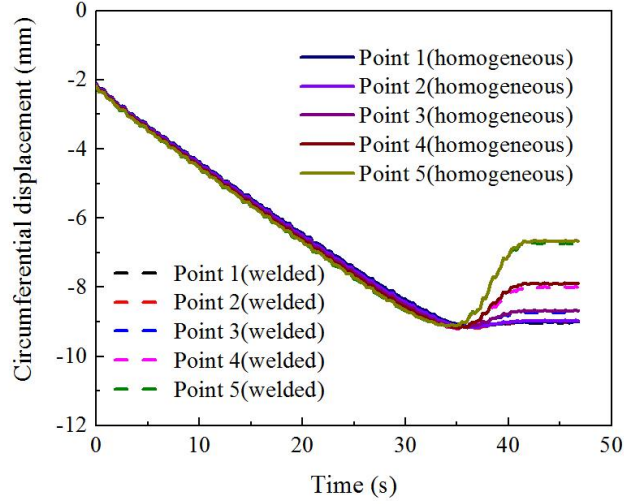


Fig. 13 The circumferential displacement curves of tracked points on welded and homogeneous tubes.

3.3 Effects of processing parameters on the weld line deflection

As analyzed above, the weld line deflection is caused by the shear deformation in θ - z plane and the deflection angle (helix angle α) is determined by the final shear strain $\varepsilon_{\theta z}$ after forming stage. During forming process, the processing parameters, such as the reduction (ψ_t), feed rate (f) and attack angle (α_R), may affect the shear deformation in θ - z plane, thus present significant impacts on the deflection angle. In this section, the effects of processing parameters on the shear strain $\varepsilon_{\theta z}$ and deflection angle were investigated by the combination of FE simulation and orthogonal experiment design. The orthogonal experiment design is a widely used sampling strategy, which can study the effect of many factors simultaneously in a single set of experiments with much fewer experiments ([Shen et al., 2016](#)). The $L_9(3^4)$ matrix was used in this work. The considered factors and their levels are given in [Table 3](#), and the designed experiment schemes are shown in [Table 4](#). After simulation, the results of deflection angle, Δ_1 and Δ_2 at outer surface were obtained and listed in [Table 4](#).

Table 3 Factors and levels of orthogonal experiment.

Factors	Level 1	Level 2	Level 3
Factor A Reduction ψ_t (%)	15	30	45
Factor B Feed rate f (mm/r)	2/3	1	4/3

Factor C Attack angle α_R (°)	20	25	30
---	----	----	----

Table 4 Orthogonal experiment schemes and simulated results of weld line deflection.

No.	ψ_t (%)	f (mm/r)	α_R (°)	Deflection angle (°)	Δ_1	Δ_2
1	15	2/3	20	4.32	0.218	0.145
2	15	1	25	4.12	0.245	0.177
3	15	4/3	30	4.31	0.261	0.190
4	30	1	30	11.48	0.461	0.278
5	30	4/3	20	11.152	0.476	0.262
6	30	2/3	25	9.646	0.414	0.230
7	45	4/3	25	18.32	0.782	0.387
8	45	2/3	30	13.93	0.642	0.382
9	45	1	20	13.52	0.680	0.430

The range analysis is applied to study the effect significance and law of factors on the target value. There are two important parameters in a range analysis, i.e., K_{ji} and R_j , whose detailed calculation processes can be found in the work of Wu et al. (2011). Fig. 14 shows the range analysis results on the deflection angle. Comparing the range values of different factors (Fig. 14(a)), it can be found that ψ_t is the most significant factor for deflection angle and f is the second significant factor. It can be observed from Fig. 14(b) that both of the increases of ψ and f will increase the deflection angle. This is because the increases of ψ_t and f need larger roller action force, which will intensify the propelling effect of roller and then improve the shear deformation in θ - z plane. As shown in Figs. 15 and 16, both of Δ_1 and Δ_2 are mainly affected by ψ_t , which increase with ψ_t and f . It should be noted that the magnitude of final shear strain (Δ_1 - Δ_2) also increases with ψ_t and f . Thus, the deflection angle increases with ψ_t and f .

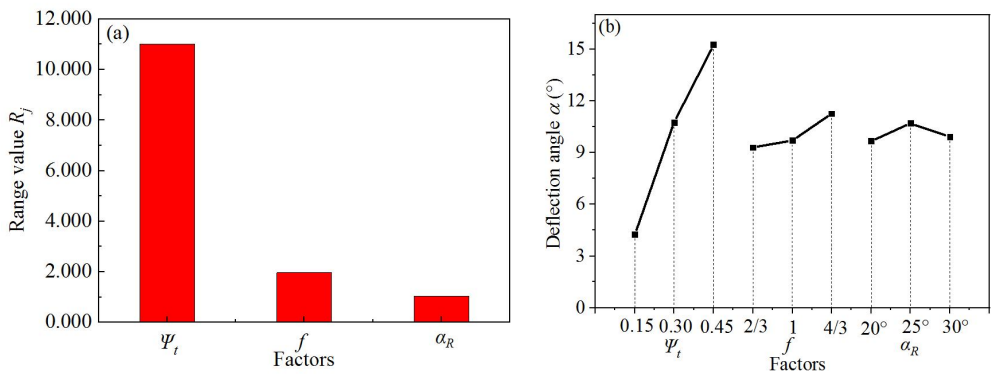


Fig. 14 Range analysis results on the weld line deflection degree: (a) range values of different factors; (b) the relationship between deflection degree and levels of different factors.

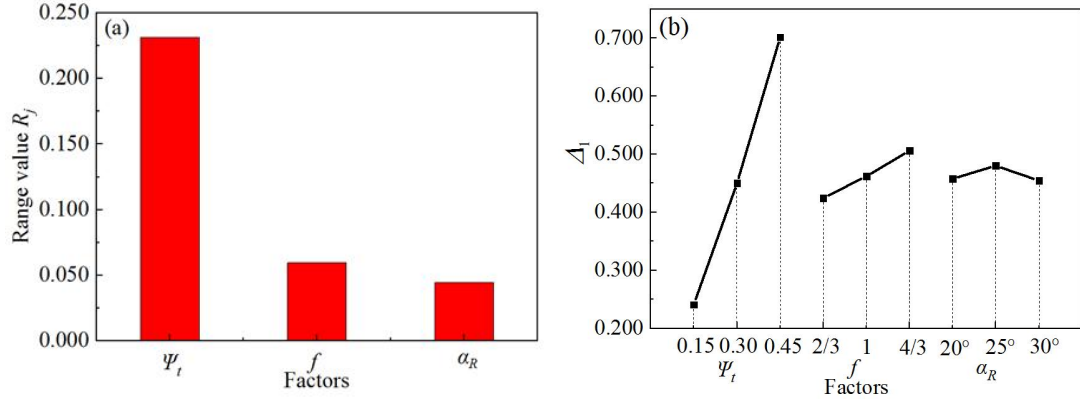


Fig. 15 Range analysis results on the negative shear Δ_1 : (a) range values of different factors; (b) the relationship between Δ_1 and levels of different factors.

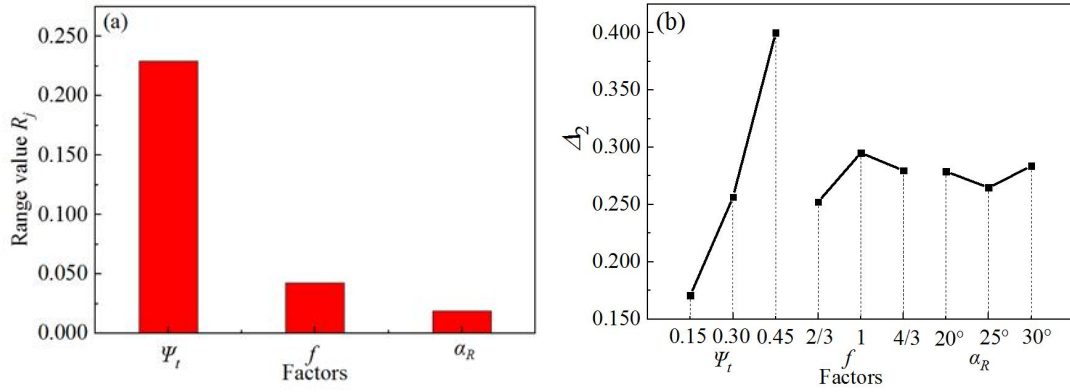


Fig. 16 Range analysis results on the positive shear Δ_2 : (a) range values of different factors; (b) the relationship between Δ_2 and levels of different factors.

4. Control method of weld line deflection

Controlling the weld line deflection is of great significance to improve the material utilization and enlarges the effective size in manufacturing large-scale integral blank by the three-step integrated process (Fig. 1). As described in Section 3, the shear deformation in θ - z plane is the essential reason responsible for the weld line deflection. Thus, how to eliminate the shear strain $\varepsilon_{\theta z}$ is the key problem for controlling the weld line deflection. To this end, two methods with different ideas will be introduced as follows.

4.1 Control by two-pass spinning with reverse rotation directions

The main idea of this method is conducting two spinning passes with opposite rotation directions of workpiece to obtain opposite shear deformation, thus the shear strains and deflections in two passes can be canceled out, as shown in Fig. 17.

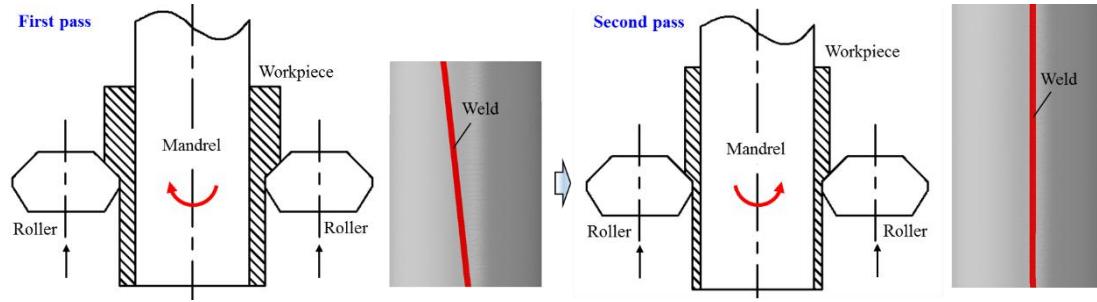


Fig. 17 The schematic of controlling the weld line deflection by two-pass spinning with reverse rotation direction.

The key of this approach is achieving the same magnitude of deflection angle in two spinning passes. As mentioned in Section 3.3, the weld deflection angle is strongly dependent on the processing parameters such as the reduction (ψ_t), feed rate (f), billet geometry and roller geometry, etc. Due to the coupling effects of these processing parameters, it is difficult to establish a quantitative prediction model of deflection angle, which brings great challenge to control the deflection angle by adjusting processing parameters. In order to straighten the weld line, it is necessary to conduct repeated trial and error to obtain suitable matching of parameters in two spinning passes. In addition, once the material and geometry of target component were changed, the processing parameters in two spinning passes must be determined again. As a result, this approach requires at least two spinning passes and laborious processing design, moreover, presents poor universality. Thus, this is a feasible but not preferred method to control the weld line deflection.

4.2 Control by applying circumferential constraint on the workpiece

To overcome the disadvantages of complexity and poor universality of the above method, we propose a new convenient method. Its main idea is controlling the circumferential deflection by a mechanical constraint directly. As shown in Fig. 18(a), the tube tail is constrained in circumferential direction by a clamping device in this method, which is different from the normal flow forming with tube tail being in free state. Here, we call this new type of flow forming as circumferential-constrained flow forming.

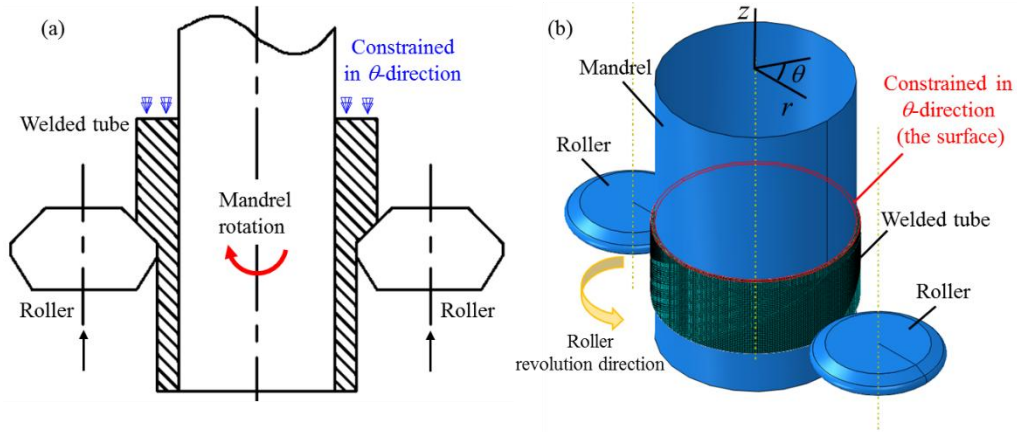


Fig. 18 The schematic (a) and FE model (b) of controlling the weld line deflection by applying circumferential constraint on the workpiece.

To analyze the roles of circumferential constraint in deformation characteristics and weld line deflection, the FE model of circumferential-constrained flow forming was developed, as shown in Fig. 18(b). Except for the circumferential constraint at tube tail, all the FE modelling parameters are the same as those of the normal FE model (Section 2.1). Fig. 19 compares the typical shear strain $\varepsilon_{\theta z}$ evolutions of a certain tracked point in the circumferential-constrained and normal non-constrained flow forming. It can be seen that both of them experience two stages of shear deformation in θ - z plane in the opposite directions during forming stage. And the durations of the negative and positive shear deformation processes are both the same for two conditions. However, the magnitudes of the negative and positive shear strain (Δ_1' and Δ_2') are almost equal at the circumferential-constrained condition. They cancel each other out leaving the $\varepsilon_{\theta z}$ after forming stage approach 0, which is quite different from that of non-constrained condition. This is because whether the tracked point locates in the negative or positive shear deformation region, their constraints at the far-end of tube are almost the same. Thus, very close magnitudes of the negative and positive shear strain are achieved. This means that the straight weld line can be obtained after circumferential-constrained flow forming. Fig. 20 shows the simulated forming results after a single-pass spinning to 30% reduction under circumferential-constrained and normal non-constrained conditions, respectively. It can be seen that a straight weld line is obtained under circumferential-constrained flow forming (Fig. 20(a)). While, the weld line is severely deflected 9.63° after the normal flow forming, whose circumferential deflection distance reaches 67.26mm when the spinning length of tube is 400mm. In addition, it can be seen from the comparison in Fig. 20 that no detrimental results are produced due to the circumferential constraint

on workpiece. These results validate the proposed new method to control the weld line deflection.

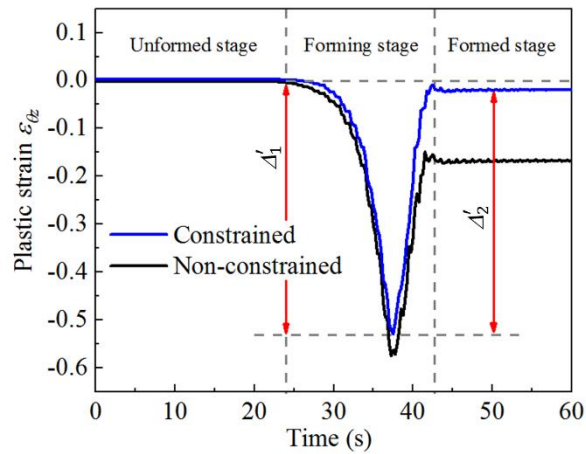


Fig. 19 Typical shear strain $\varepsilon_{\theta z}$ evolutions of a certain tracked point in the circumferential-constrained and normal non-constrained flow forming.

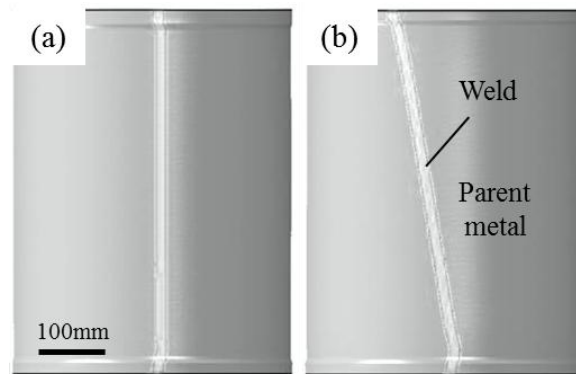


Fig. 20 Forming results after single-pass spinning to 30% reduction under different conditions: (a) circumferential-constrained; (b) normal non-constrained.

As for the clamping device to apply circumferential constraint, there may be many feasible schemes. In this work, we propose a scheme shown in Fig. 21. Its main feature is fixing the tube tail with a chuck and then fixing the chuck to two axial guideways in mandrel to restrict its circumferential rotation. During deformation, the tube can be elongated through the axial movement of guideways but restricted in the circumferential direction, which provides a feasible scheme to apply circumferential constraint on the tube tail.

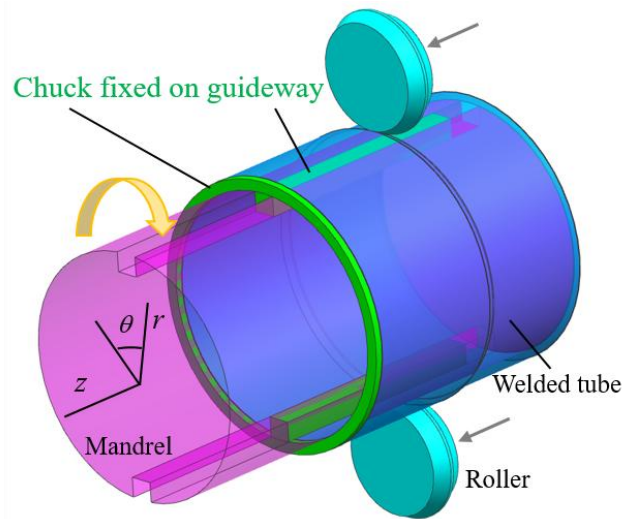


Fig. 21 Schematic of the designed clamping device to apply circumferential constraint on the tube tail.

The above analyses suggest that the proposed control method by applying circumferential constraint can change the circumferential deformation characteristics and thus eliminate the shear strain $\varepsilon_{\theta z}$ and weld line deflection during flow forming. Moreover, it is realized by mechanical constraint device, thus does not depend on the processing parameters, which can avoid the tedious processing design. Meanwhile, the circumferential-constrained method can eliminate the weld line deflection in single spinning pass for tubes with various materials and geometries. These characteristics make the circumferential-constrained flow forming become a preferred method with high efficiency and good universality for controlling the weld line deflection.

5. Conclusions

In this paper, the characterization, mechanism and control method of weld line deflection in the flow forming of an aluminum alloy welded tube were investigated. The following conclusions can be drawn:

(1) During flow forming, the weld line was deflected and mainly displayed in the rigid rotation of unformed region. Finally, the deformed weld line turns into a helix with the reverse helix orientation relative to the helical trajectory of roller on workpiece. The helix angle can be defined as deflection angle to evaluate the deflection degree.

(2) The weld line deflection is caused by the synthetical effects of shear deformation in θ - z and r - θ planes. The simple shear deformation in θ - z plane in forming region is the underlying reason for weld line deflection. The shear strain $\varepsilon_{\theta z}$ nearly equals to the deflection angle. The shear deformation in r - θ plane ($\varepsilon_{r\theta}$) leads to the deflection distance at inner surface a little larger than that of outer surface, but makes little difference on the deflection angles of two surfaces. Reduction and feed rate are the first

and second significant factor for the deflection angle of weld line, while the attack angle has little effect. The deflection angle increases with the reduction and feed rate.

(3) Conducting two-pass spinning with the reverse rotation directions of workpiece is feasible to obtain opposite shear deformation in θ - z plane. Moreover, through rigorous processing design, the shear strain $\varepsilon_{\theta z}$ in two passes can be canceled out leaving a straight weld line. A more convenient method by applying circumferential constraint on the tube tail is proposed to control the deflection. It can change the circumferential deformation characteristics, thus eliminate the shear strain $\varepsilon_{\theta z}$ and deflection in single spinning pass for tubes with various materials and geometries. Comparatively, the second method possesses higher efficiency and better universality.

(4) The existence of weld line has little effect on the circumferential deflection comparing to the homogeneous tube, which suggests the circumferential deflection is an intrinsic phenomenon in the flow forming of tubes. Thus, the results provide well explanation and control method for the intrinsic circumferential deflection (or called as twisting) in the flow forming.

Acknowledgments

The authors would acknowledge the funding support from the National Science Fund for Distinguished Young Scholars of China (No. 51625505) and the Key Program Project of the Joint Fund of Astronomy and National Natural Science Foundation of China (No. U1537203), National Natural Science Foundation of China (No. 51875467), the Hong Kong Scholar Program (No. XJ2018010) and the Young Elite Scientists Sponsorship Program by CAST (No. 2018QNRC001).

References

- Fu, M.W., 2016. Design and Development of Metal Forming Processes and Products Aided by Finite Element Simulation, first ed. Springer-Verlag London Ltd.
- Heo, Y.M., Wang, S.H., Kim, H.Y., Seo, D.G., 2001. The effect of the drawbead dimensions on the weld-line movements in the deep drawing of tailor-welded blanks. *J. Mater. Process. Technol.* 113, 686-691.
- Kwiatkowski, L., Tekkaya, A.E., Kleiner, M., 2013. Fundamentals for controlling thickness and surface quality during dieless necking-in of tubes by spinning. *CIRP Annals- Manufacturing Technology.* 62, 299-302.
- Liu, J., Gao, H., Fakir, O.E., Wang, L., Lin, J., 2016. Hot stamping of AA6082 tailor welded blanks: experiment and FE simulation. *Manufacturing Review.* 3, 8-8.

- Mohebbi, M.S., Akbarzadeh, A., 2010. Experimental study and FEM analysis of redundant strains in flow forming of tubes. *J. Mater. Process. Technol.* 210, 389-395.
- Shan D.B., Yang G.P., Xu W.C., 2009. Deformation history and the resultant microstructure and texture in backward tube spinning of Ti-6Al-2Zr-1Mo-1V, *Journal of Materials Processing Technology* 209 5713-5719.
- Shen, Q., Zheng, Y., Li, S., Ding, H., Xu, Y., Zheng, C., Thern, M., 2016. Optimize process parameters of microwave-assisted EDTA method using orthogonal experiment for novel BaCoO 3- δ perovskite. *J. Alloys Compd.* 658, 125-131.
- Shinde, H., Mahajan, P., Singh, A.K., Singh, R., Narasimhan, K., 2016. Process modeling and optimization of the staggered backward flow forming process of maraging steel via finite element simulations. *Int. J. Adv. Manuf. Technol.* 87, 1-14.
- Thiel, C., Voss, J., Martin, R.J., Neff, P., 2019. Shear, pure and simple. *International Journal of Non-Linear Mechanics.* 112, 57-72.
- Wang, A., Liu, J., Gao, H.X., Wang, L.L., Masen, M., 2017. Hot stamping of AA6082 tailor welded blanks: experiments and knowledge-based cloud- finite element (KBC-FE) simulation. *J. Mater. Process. Technol.* 250, 228-238.
- Wang, X.X., Zhan, M., Fu, M.W., Gao, P.F., Guo, J., Ma, F., 2018. Microstructure evolution of Ti-6Al-2Zr-1Mo-1V alloy and its mechanism in multi-pass flow forming. *J. Mater. Process. Technol.* 261, 86-97.
- Wu, X., Leung, D.Y.C., 2011. Optimization of biodiesel production from camelina oil using orthogonal experiment. *Appl. Energy.* 88, 3615-3624.
- Xu, W.C., Zhao, X.K., Ma, H., Shan, D.B., Lin, H.L., 2016. Influence of roller distribution modes on spinning force during tube spinning. *Int. J. Mech. Sci.* 113, 10-25.
- Xu, Y., Zhang, S.H., Li, P., Yang, K., Shan, D.B., Lu, Y., 2001. 3D rigid-plastic FEM numerical simulation on tube spinning. *Journal of Materials Processing Technology.* 113, 710-713.
- Xue, K.M., Li, P., Lu, Y., Kawai, K., 2001. Influence of process parameters on tangential strain in tube spinning. *J. Harbin Ins Titute of Technol.* 33, 86-88.
- Yang, H., Li, H., Zhan, M., 2010. Friction role in bending behaviors of thin-walled tube in rotarydraw-bending under small bending radii. *J. Mater. Process. Technol.* 210, 2273-2284.
- Zhang, C., 2012. Research of the warm forming in V-shape free bending of 5A06 Aluminum alloy

tailor welded blanks, Hefei University of Technology.

Zhang, Y.L., Wang, F.H., Dong, J., Jin, L., Liu, C., Ding, W.J., 2017. Grain refinement and orientation of AZ31B magnesium alloy in hot flow forming under different thickness reductions. *J. Mater. Sci. Technol.* 34, 1091-1102.